GRP78 is a novel receptor initiating a vascular barrier protective response to oxidized phospholipids

Anna A. Birukova[a,*], Patrick A. Singleton[a,*], Grzegorz Gawlak[a], Xinyong Tian[a], Tamara Mirzapoiazova[a], Bolot Mambetsariev[a], Oleksii Dubrovskyi[a], Olga V. Oskolkova[a,b], Valery N. Bochkov[b], and Konstantin G. Birukov[a]

[a]Lung Injury Center, Section of Pulmonary and Critical Care, Department of Medicine, Division of Biomedical Sciences, University of Chicago, Chicago, IL 60637; [b]Department of Vascular Biology and Thrombosis Research, Medical University of Vienna, 1090 Vienna, Austria

ABSTRACT **Vascular integrity and the maintenance of blood vessel continuity are fundamental features of the circulatory system maintained through endothelial cell–cell junctions. Defects in the endothelial barrier become an initiating factor in several pathologies, including ischemia/reperfusion, tumor angiogenesis, pulmonary edema, sepsis, and acute lung injury. Better understanding of mechanisms stimulating endothelial barrier enhancement may provide novel therapeutic strategies. We previously reported that oxidized phospholipids (oxidized 1-palmitoyl-2-arachidonoyl-*sn*-glycero-3-phosphocholine [OxPAPC]) promote endothelial cell (EC) barrier enhancement both in vitro and in vivo. This study examines the initiating mechanistic events triggered by OxPAPC to increase vascular integrity. Our data demonstrate that OxPAPC directly binds the cell membrane–localized chaperone protein, GRP78, associated with its cofactor, HTJ-1. OxPAPC binding to plasma membrane–localized GRP78 leads to GRP78 trafficking to caveolin-enriched microdomains (CEMs) on the cell surface and consequent activation of sphingosine 1-phosphate receptor 1, Src and Fyn tyrosine kinases, and Rac1 GTPase, processes essential for cytoskeletal reorganization and EC barrier enhancement. Using animal models of acute lung injury with vascular hyperpermeability, we observed that HTJ-1 knockdown blocked OxPAPC protection from interleukin-6 and ventilator-induced lung injury. Our data indicate for the first time an essential role of GRP78 and HTJ-1 in OxPAPC-mediated CEM dynamics and enhancement of vascular integrity.**

Monitoring Editor
Alpha Yap
University of Queensland

Received: Dec 17, 2013
Revised: May 2, 2014
Accepted: May 6, 2014

This article was published online ahead of print in MBoC in Press (http://www.molbiolcell.org/cgi/doi/10.1091/mbc.E13-12-0743) on May 14, 2014.

*These are co–first authors.

Address correspondence to: Konstantin Birukov (kbirukov@medicine.bsd.uchicago.edu).

Abbreviations used: BAL, bronchoalveolar lavage; CEM, caveolin-enriched microdomain; DMPS, oxidation-resistant phosphatidyl serine; EC, endothelial cell; ER, endoplasmic reticulum; HPAEC, human pulmonary artery endothelial cells; HTV, mechanical ventilation at high tidal volume; OxPAPC, oxidized 1-palmitoyl-2-arachidonoyl-*sn*-glycero-3-phosphocholine; OxPAPS, oxidized 1-palmitoyl-2-arachidonoyl-*sn*-glycero-3-phosphoserine; OxPL, oxidized phospholipid; S1P-R1, sphingosine 1-phosphate receptor 1; TER, transendothelial electrical resistance.

INTRODUCTION

The effects of oxidized phospholipids (OxPLs) described in vitro and in vivo demonstrate their relevance to different pathologies, acute inflammation, ischemia/reperfusion injury, atherosclerosis, lung injury, and many other conditions (Bochkov *et al.*, 2010). Besides their role as pathogenic factors, full-length products of phospholipid oxidation, such as oxidized 1-palmitoyl-2-arachidonoyl-*sn*-glycero-3-phosphocholine (OxPAPC) and oxidized 1-palmitoyl-2-arachidonoyl-*sn*-glycero-3-phosphoserine (OxPAPS), exhibit potent barrier-enhancing and anti-inflammatory effects in vitro and in vivo (Walton *et al.*, 2003; Birukova *et al.*, 2007a; Oskolkova *et al.*, 2010). Single intravenous injection of OxPAPC in animal models inhibited lung inflammation and lung vascular leak induced by intratracheal administration of bacterial lipopolysaccharide (Ma *et al.*, 2004; Nonas *et al.*, 2006) or mechanical ventilation at high tidal volume (HTV; Nonas *et al.*, 2008).

We described potent barrier-enhancing effects of OxPAPC on vascular endothelium. The signaling mechanism involved recruitment of sphingosine 1-phosphate receptor-1 (S1P-R1) to the caveolin-enriched microdomains (CEMs, also known as lipid rafts or caveoli) and activation of serine/threonine kinases mammalian target of rapamycin (mTOR) and phosphoinositide 3-kinase (PI3K) and Rac-specific nucleotide exchange factors Tiam1 and Vav2, which stimulated Rac1 GTPase signaling to cytoskeleton and cell junctions (Singleton *et al.*, 2009; Birukova *et al.*, 2011). A number of OxPL receptors (PAF receptor, CD36 scavenger receptor BI, prostaglandin receptor EP2, vascular endothelial growth factor [VEGF] receptor-2, S1P-R1) have been identified that mediate different cellular effects of OxPLs, such as modulation of innate immunity, activation of antioxidant gene expression, VEGF expression and signaling, expression of proatherosclerotic factors, proangiogenic effects, and increased permeability and OxPL uptake (Ishii *et al.*, 2003; Bluml *et al.*, 2005; Salomon, 2005; Imai *et al.*, 2008; Bochkov *et al.*, 2010). However, the primary receptor(s) mediating OxPAPC-induced endothelial cell (EC) barrier enhancement remain elusive.

GRP78 is a multifunctional regulator of endoplasmic reticulum (ER) homeostasis and stress response. It was initially identified as a key component of the cellular stress pathway induced by accumulation of unfolded proteins. GRP78 is mainly located in the ER, where it binds denatured or incorrectly folded polypeptides and initiates a cascade of protective reactions helping the cell to survive under conditions of stress induced by protein overload (He *et al.*, 2011), viral infection (Shi-Chen Ou *et al.*, 2011; Thongtan *et al.*, 2012), and so on. Alterations in GRP78 tissue levels or activity have been implicated in cancer, immune regulation, aging, Alzheimer disease, and other diseases associated with ER stress (Misra *et al.*, 2005; Pfaffenbach and Lee, 2011; Wei *et al.*, 2012; Soejima *et al.*, 2013).

HTJ-1, or its mouse homologue MTJ-1, is a partner of GRP78 in ER protein quality control (Chevalier *et al.*, 2000). In addition to its role as an ER-localized cochaperone involved in the unfolded protein response, a second important function of HTJ-1/MTJ-1 is the translocation and anchoring of GRP78 to the cell plasma membrane, where GRP78 assumes a novel role. Cell surface–expressed GRP78 functions as a signal-transducing receptor or coreceptor for soluble ligands such as α_2-macroglobulin (Misra *et al.*, 2005), tumor differentiation factor (Sokolowska *et al.*, 2012), and vaspin (Nakatsuka *et al.*, 2012), as well as for glycosylphosphatidylinositol-anchored proteins—for example, T-cadherin (Philippova *et al.*, 2008) and teratocarcinoma-derived growth factor 1 (Cripto; Shani *et al.*, 2008). The present study examines a role of surface-expressed GRP78 as an initiator of the OxPAPC-mediated barrier-enhancing signaling cascade in vitro and in vivo. Our data support the notion that GRP78 functions as a receptor for OxPLs that is critically important for their barrier-protective effects.

RESULTS

Inhibition of the cell membrane–associated GRP78 pool attenuates OxPAPC-induced EC barrier enhancement and F-actin remodeling

Inhibition of cell membrane–associated GRP78 was achieved by EC preincubation with GRP78- blocking antibody or by small interfering RNA (siRNA)–induced knockdown of GRP78 cofactor, HTJ-1, essential for GRP78 translocation to the cell membrane (Chevalier *et al.*, 2000). Because cytosolic and endoplasmic reticulum–associated pools of GRP78 are important for other cell functions (Li and Lee, 2006; Wei *et al.*, 2012), global knockdown of GRP78 was not used in this study. GRP78-blocking antibody binds the extracellular C-terminal GRP78 domain and blocks its interactions with extracellular ligands (Philippova *et al.*, 2008; Misra *et al.*, 2009). This antibody-attenuated increase in transendothelial electrical resistance (TER) reflects the OxPAPC-induced barrier enhancement response, whereas control immunoglobulin G (IgG) antibody is without effect (Figure 1A). Similarly, inhibition of GRP78 targeting to the cell membrane by HTJ-1 knockdown abolished OxPAPC-induced barrier enhancement (Figure 1B). In control experiments, HTJ-1 knockdown did not affect EC barrier enhancement induced by the prostacyclin stable analogue iloprost (Figure 1C), known to act via a distinct pathway mediated by prostacyclin receptor IP (Bos *et al.*, 2004). These results demonstrate specific involvement of the HTJ-1-GRP78 mechanism in the OxPAPC-induced EC barrier enhancement. OxPAPC-induced changes in TER were associated with increased EC monolayer barrier properties reflected by decreased penetration of fluorescein isothiocyanate (FITC)–labeled avidin through intercellular junctions, as measured by XPerT permeability assay (Dubrovskyi *et al.*, 2013; Figure 1EF). This EC barrier enhancement response was attenuated by HTJ1 depletion.

GRP78–HTJ-1 association is stimulated by OxPAPC

GRP78 and HTJ-1 are expressed in microvascular and macrovascular endothelial cells (Figure 2A). Stimulation with 10 µg/ml OxPAPC increased GRP78–HTJ-1 association in cells, as determined by coimmunoprecipitation assay (Figure 2B). Of note, the oxidation-resistant phospholipid dimyristoylphosphatidylcholine (DMPC) had no effect on GRP78–HTJ-1 association.

GRP78 localizes at cell membrane and directly interacts with OxPAPC and OxPAPS

The foregoing experiments suggested the role of GRP78 in initiating the OxPAPC-induced EC cytoskeletal remodeling and barrier response. Direct interaction between GRP78 and OxPLs was tested by several approaches. First, cells preincubated with OxPAPC or nonoxidized control (DMPC) were used for immunoprecipitation with anti-OxPAPC antibody EO6 (Friedman *et al.*, 2002). Cell incubation with OxPAPC significantly increased GRP78 content in EO6 immunoprecipitates (Figure 2C). In the lipid native gel mobility shift assay, interaction with phospholipid bearing a phosphoserine polar head group will increase net protein negative charge, leading to increased electrophoretic mobility of the GRP78xphospholipid complex under nondenaturing conditions. GRP78 preincubation with OxPAPS increased electrophoretic mobility of GRP78 (Figure 2D, left). Preincubation with oxidation-resistant phosphatidyl serine (DMPS) did not cause a GRP78 mobility shift. Monoclonal antibody E06 (Horkko *et al.*, 1999) recognizes OxPAPC but not OxPAPS or nonoxidized PAPC species and may be a useful tool for detection of OxPAPC complexes. Purified GRP78 was preincubated with control buffer, OxPAPC, OxPAPS, or their respective nonoxidizable analogues, DMPC and DMPS. Immunoblotting with E06 monoclonal antibody, which reacts with oxidized phosphatidyl choline species (Friedman *et al.*, 2002), revealed strong immunoreactivity of purified recombinant GRP78 preincubated with OxPAPC but not with any other phospholipid (Figure 2D, right).

Interaction of recombinant GRP78 with phospholipids immobilized on plastic was further tested by enzyme-linked immunosorbent assay (ELISA). Because test experiments showed low adsorption of OxPAPC to polystyrene plates (unpublished data), for ELISAs, we used OxPAPS, which, similarly to OxPAPC, causes a barrier-protective response in pulmonary EC (Birukova *et al.*, 2007a). The oxidation-resistant PAPS analog DMPS was used as negative control. Human recombinant GRP78 efficiently interacted with OxPAPS but not with DMPS (Figure 2E, left). Similar experiments were performed

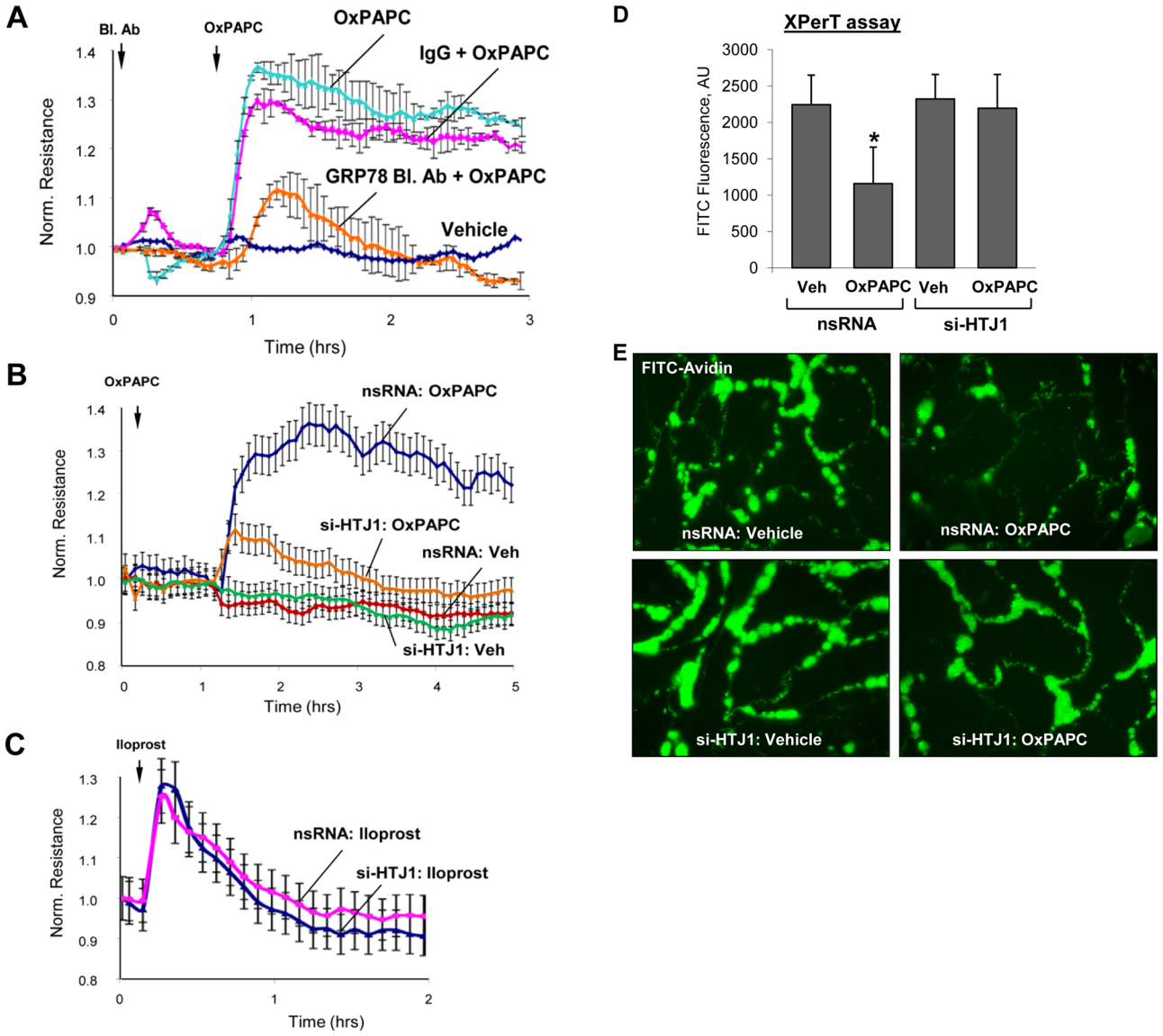

FIGURE 1: GRP78 and OxPAPC-induced EC barrier enhancement. (A) HPAECs plated on microelectrodes were treated with vehicle (IgG) or GRP78-blocking antibody (50 μg/ml), followed by OxPAPC (10 μg/ml) stimulation and TER measurements. (B) HPAECs were transfected with HTJ-1–specific siRNA or nonspecific RNA, followed by stimulation with OxPAPC and TER measurements. (C) HTJ-1 knockdown did not affect the TER increase in HPAEC caused by iloprost (200 ng/ml). (D, E) HPAECs grown in 96-well plates (D) or on glass coverslips (E) with immobilized biotinylated gelatin (0.25 mg/ml) were transfected with HTJ1-specific siRNA or nonspecific RNA. After 72 h, the cells were stimulated with OxPAPC for 30 min, followed by addition of FITC-avidin (25 μg/ml, 3 min). Unbound FITC-avidin was removed, and FITC fluorescence was measured; *$p < 0.05$; $n = 5$.

on plates with immobilized OxPAPS incubated with EC lysates containing endogenous GRP78. GRP78 immunoreactivity was significantly higher in OxPAPS-containing wells incubated with cell lysate (Figure 2E, middle). Similar to results of ELISA with purified protein, GRP78 endogenously expressed in endothelial cells interacted with immobilized OxPAPS but not with DMPS (Figure 2E, right). Together these data demonstrate the direct interaction of OxPAPS and OxPAPC with GRP78.

GRP78 cell membrane localization was tested by an immunocytochemistry approach. Plasma membrane was counterstained with Alexa 576–conjugated wheat germ agglutinin. Confocal microscopy analysis showed that OxPAPC promoted GRP78 accumulation within the plasma membrane (Figure 3A). The OxPAPC-induced GRP78 cell surface location was further verified by in situ biotinylation of cell surface proteins in control and OxPAPC-challenged EC, and the level of biotinylated GRP78 was assessed by Western blot. Increased GRP78 biotinylation was observed in cells treated with OxPAPC (Figure 3B). Increased levels of biotinylated VE-cadherin also illustrate OxPAPC-induced activation of VE-cadherin surface expression and adherens junction dynamics. EC treatment with 10 μg/ml OxPAPC did not affect the cell surface presentation of VEGF receptor-2 (VEGFR2). In complementary experiments, the CEMs (lipid rafts) were isolated from control and OxPAPC-stimulated EC after cell surface biotin labeling, followed by GRP78 immunoprecipitation. OxPAPC treatment increased the levels of biotinylated GRP78 detected in GRP78 precipitates (Figure 3C).

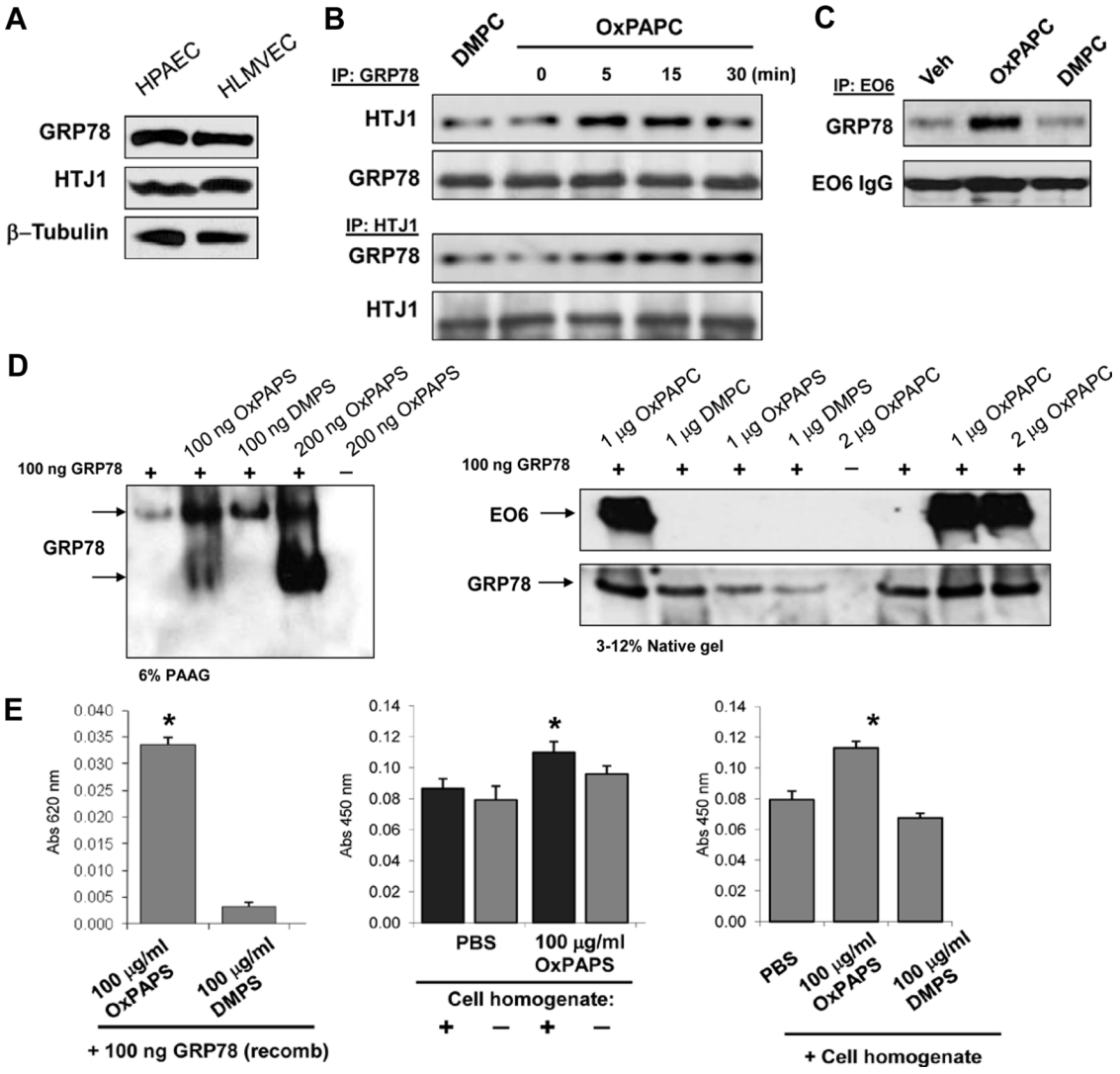

FIGURE 2: Analysis of GRP78–HTJ1 and OxPL–GRP78 interactions. (A) GRP78 and HTJ1 expression in HPAEC and human lung microvascular endothelial cells was detected by Western Blot. (B, C) GRP78 interactions were analyzed in coimmunoprecipitation assays using lysates from control or DMPC- (10 μg/ml, 15 min) or OxPAPC-stimulated (10 μg/ml) cells with antibody to GRP78 (B, top), HTJ1 (B, bottom), or EO6 antibody recognizing OxPL (C). (D) Human recombinant GRP78 was incubated with OxPAPC, OxPAPS, or their oxidation-resistant analogues DMPC or DMPS. Left, native gel electrophoresis, followed by Western blot with anti-GRP78 antibody. Shift in electrophoretic mobility of GRP78 incubated with OxPAPS, but not DMPS, indicates formation of GRP78–OxPAPS complex. Right, SDS–PAGE, followed by Western blot with EO6 antibody and reprobing with anti-GRP78 antibody. Positive EO6 immunoreactivity of GRP78 preincubated with OxPAPC indicates formation of GRP78–OxPAPC complex. (E) ELISA plates coated with OxPAPS or DMPS or control uncoated plates incubated with PBS incubated with human recombinant GRP78 (left) or HPAEC lysates (middle and right). The bound GRP78 was detected using anti-GRP78 antibody. *$p < 0.05$ vs. DMPS or PBS; $n = 4$.

OxPAPC-induced recruitment of S1P-R1 signaling complex to cell membrane caveolin-enriched microdomains is mediated by GRP78/HTJ-1

Accumulation of S1P-R1 in lipid rafts and its transactivation by Src family kinases Src and Fyn triggers the Rac-dependent mechanism of EC barrier enhancement by OxPAPC (Singleton *et al.*, 2009). However, the upstream mechanism that triggers an S1P-R1 signaling complex assembly by OxPAPC is unknown. We tested a role of OxPAPC-GRP78/HTJ-1 interaction as a molecular switch leading to S1P-R1 transactivation and EC barrier response. Cell stimulation with OxPAPC induced recruitment of S1P-R1 and phosphorylated Src, Fyn, and Rac1 to CEM, which was also accompanied by accumulation of GRP78 and HTJ-1 (Figure 4A). SiRNA-induced knockdown of HTJ-1 abolished GRP78 recruitment and assembly of S1P-R1 signaling complex in the CEM (Figure 4B). Of importance, siRNA-based knockdown of caveolin-1 or disruption of the CEM by methyl-β-cyclodextrin (MβCD) inhibited GRP78 and HTJ-1 translocation after OxPAPC treatment (Figure 4C). Of note, the endoplasmic reticulum markers calnexin and calreticulin were not detected in the CEM preparation.

We further examined the mechanism by which GRP78 initiates S1P-R1 transactivation. CEM disruption by cell pretreatment with MβCD abolished OxPAPC-induced phosphorylation of S1P-R1 at Thr-236, which reflects its activation (Lee *et al.*, 2001) but did not

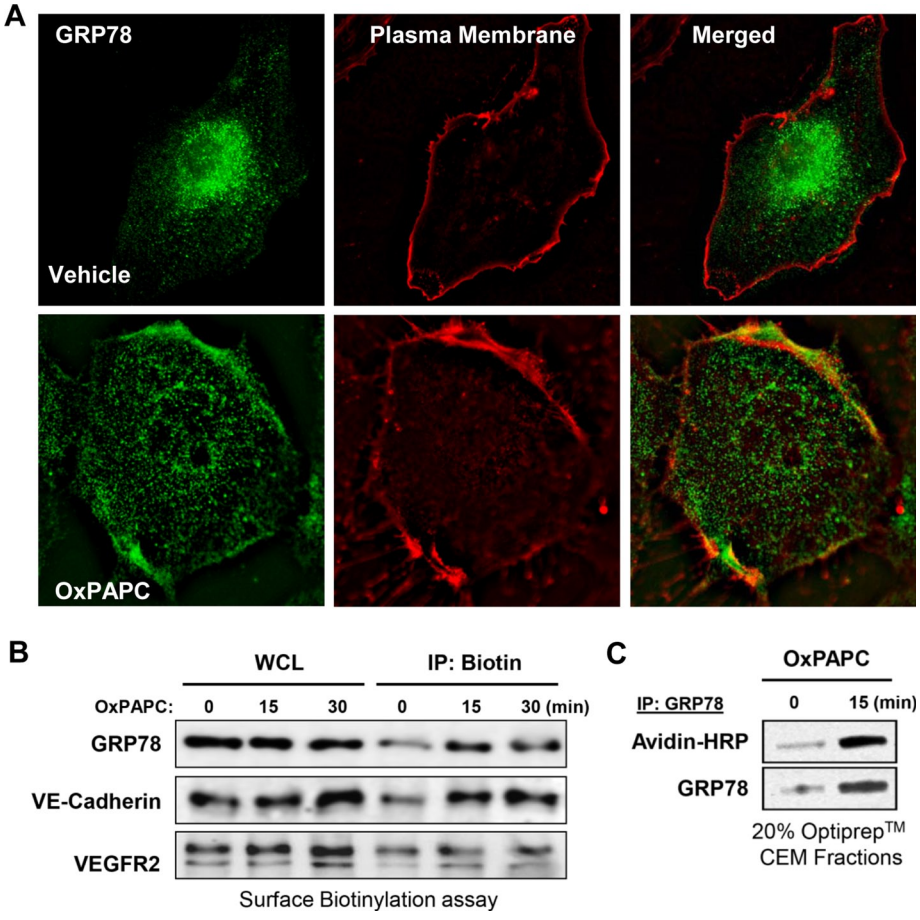

FIGURE 3: Analysis of OxPAPC-induced GRP78 membrane translocation. (A) Endothelial cells grown on glass coverslips were stimulated with vehicle of OxPAPC (10 μg/ml, 15 min), followed by immunofluorescence labeling of GRP78 (green) and plasma membrane with wheat germ agglutinin (red). Merged images show GRP78 colocalization with plasma membrane labeled by wheat germ agglutinin (yellow). (B, C) Cells were stimulated with OxPAPC for indicated periods of time, and cell surface proteins were labeled with Sulfo-NHS-SS-Biotin. Biotinylated proteins were collected using streptavidin-agarose and evaluated by Western blot (B). CEM fractions (20% OptiPrep layer) were isolated, followed by GRP78 immunoprecipitation and detection of biotinylated GRP78 in precipitates using avidin-HRP–labeled antibody (C).

affect OxPAPC-induced accumulation of HTJ1 and GRP78 in the plasma membrane (Figure 4D). On the other hand, immunoprecipitation of GRP78 from membrane fractions showed that OxPAPC stimulation caused both the GRP78–S1P-R1 association and S1P-R1 transactivation, whereas CEM disruption by MβCD prevented S1P-R1 transactivation but did not affect OxPAPC-induced GRP78–S1P-R1 complex formation (Figure 4E). These results suggest that OxPAPC recruits GRP78 to the plasma membrane and stimulates GRP78–S1P-R1 interactions. However, further S1P-R1 transactivation requires targeting of the GRP78–S1P-R1 complex to the CEM domain of the plasma membrane.

HTJ-1 knockdown abolishes activation of Rac signaling and dynamic remodeling of cortical cytoskeleton induced by OxPAPC

Disruption of GRP78–HTJ-1 complex by HTJ-1 knockdown abolished GRP78 recruitment to the cell membrane induced by OxPAPC and suppressed Rac-mediated membrane accumulation of actin cytoskeletal regulatory protein cortactin (Figure 5A). These results are consistent with the key role of HTJ-1 in OxPAPC-induced targeting of GRP78 to the cell membrane. Direct analysis of Rac activity showed inhibition of OxPAPC-induced Rac activation in cells with HTJ-1 knockdown (Figure 5B).

Activation of Rac1 induces cortactin localization in lamellipodia and podosomes (Head *et al.*, 2003) and regulates actin dynamics. In turn, impaired reestablishment of EC monolayer integrity in cells with inhibited Rac1 is accompanied by suppressed cortactin peripheral localization and decreased cortactin tyrosine phosphorylation (Birukova *et al.*, 2012a). siRNA-induced knockdown of Rac-specific guanine nucleotide exchange factors Tiam1 and βPIX abolished OxPAPC-induced activation of Rac and its effector kinase PAK1 and attenuated OxPAPC-induced peripheral translocation of cortactin, peripheral actin cytoskeletal enhancement and EC barrier protective response (Birukova *et al.*, 2007b). These data demonstrate a role of OxPAPC-induced cortactin phosphorylation and peripheral translocation in the mechanisms of OxPAPC-induced EC barrier enhancement. HTJ-1 knockdown (Figure 5C) or cell pretreatment with GRP78-blocking antibody (Figure 5D) attenuated OxPAPC-induced site-specific phosphorylation of the Src and Rac targets PAK1 and cortactin.

Enhancement of the cortical actin cytoskeleton is essential for barrier-protective effects of OxPAPC (Birukova *et al.*, 2007b). Cortactin is an actin-binding protein that mediates Rac-dependent cortical actin polymerization (Weed and Parsons, 2001), and its accumulation at the cell periphery indicates formation of new F-actin networks. Pulmonary EC expressing green fluorescent protein (GFP)–tagged cortactin were depleted of HTJ-1 using specific siRNA, and OxPAPC-induced peripheral accumulation of GFP-cortactin reflecting cytoskeletal enhancement was monitored using live-cell microscopy. OxPAPC stimulation of control EC treated with nonspecific siRNA caused peripheral accumulation of GFP-cortactin observed after 1–15 min of OxPAPC treatment (Figure 6A), whereas depletion of HTJ-1 by specific siRNA abolished this effect (Figure 6B). OxPAPC-induced activation of peripheral cortactin dynamics was linked to enlargement of the peripheral F-actin rim (Figure 6C). Knockdown of HTJ-1 (Figure 6C, top) or incubation with GRP78 blocking antibody (Figure 6C, bottom) prevented OxPAPC-induced cytoskeletal remodeling.

Knockdown of mouse HTJ-1 homologue (MTJ-1) attenuates OxPAPC's protective effects in animal models of acute lung injury

Inhibition of GRP78 membrane signaling by the knockdown of MTJ-1, the mouse homologue of HTJ-1, blunted lung-protective effects of OxPAPC in animal models of acute lung injury (ALI). Endogenous MTJ-1 was depleted in mouse lungs using the siRNA approach. Lung-specific knockdown of MTJ-1 was confirmed by real time (RT)-PCR analysis of lung samples and Western blot analysis of lung, heart, liver, and kidney tissues (Figure 7A). In the interleukin-6

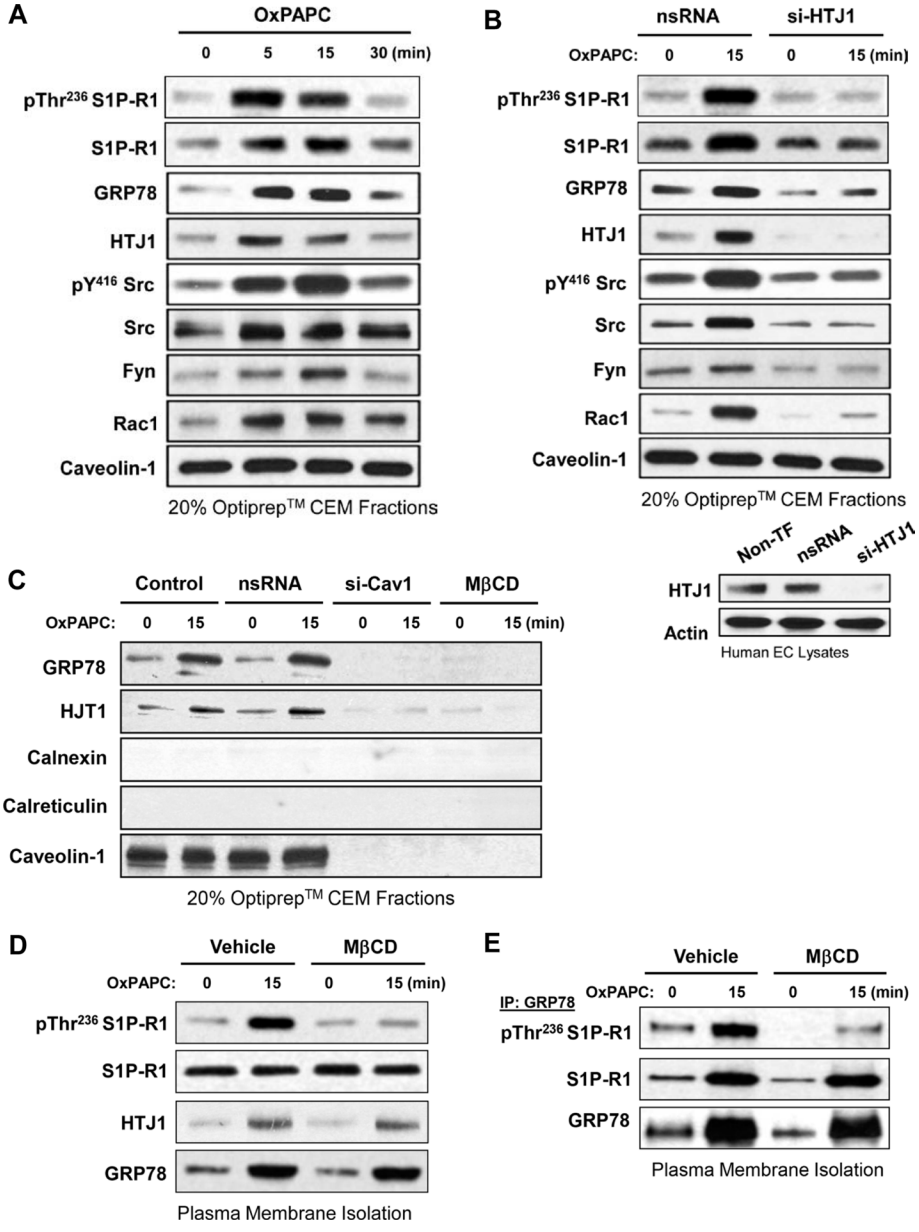

FIGURE 4: Effect of HTJ1 knockdown and MβCD treatment on OxPAPC-induced activation of signaling complex in the CEMs. (A) CEM fractions (20% OptiPrep layer) were isolated from HPAECs treated with 10 μg/ml OxPAPC. S1P-R1, GRP78, HTJ1, Src, Fyn, phospho-Src family kinases, Rac1, and caveolin as a CEM marker and detected by Western blot. (B) HPAECs treated with nonspecific or HTJ1-specific siRNA were stimulated with OxPAPC (10 μg/ml, 15 min), and CEM fractions were isolated. Accumulation of GRP78, HTJ1, Src, Fyn, Rac1, and increased phosphorylation of phospho-Src family kinases in CEM fractions was detected by Western blot. Bottom, verification of HTJ1 depletion by specific siRNA. (C) HPAECs treated with nonspecific siRNA, caveolin-1–specific siRNA, or MβCD (2 mM) were stimulated with OxPAPC, followed by isolation of CEM fractions. Accumulation of GRP78, HTJ1, calnexin, and calreticulin was detected by Western blot analysis. Bottom, verification of caveolin-1 depletion. (D, E) HPAECs treated with vehicle or MβCD (2 mM) were stimulated with OxPAPC (10 μg/ml, 15 min), followed by (D) isolation of plasma membrane fractions. Transactivation of S1P-R1 was evaluated by increased Thr-236 phosphorylation levels. Total S1P-R1, HTJ1, and GRP78 in plasma membrane fractions were detected by Western blot or (E) immunoprecipitation of GRP78 from membrane fractions. GRP-78–S1P-R1 association and S1P-R1 transactivation were monitored by Western blot.

(IL-6) model of ALI described previously (Birukova *et al.*, 2012b), mice were treated with nonspecific or MTJ-1–specific siRNA for 72 h, followed by intratracheal injection of IL-6 with or without OxPAPC treatment. At 24 h, collection of bronchoalveolar lavage (BAL) fluid was performed as described in *Materials and Methods*. IL-6 instillation significantly increased BAL protein concentration and cell count in untreated controls or mice treated with nonspecific RNA (Figure 7, B and C). These parameters were attenuated by OxPAPC administration (Figure 7B). In contrast, MTJ-1 knockdown abolished protective effects of OxPAPC against protein and cell accumulation in the BAL of the IL-6–treated group (Figure 7C). The effects of OxPAPC on the IL-6-induced lung vascular leak in control and MTJ1 knockdown mice were also evaluated by measurements of Evans blue extravasation into the lung tissue. OxPAPC significantly reduced IL-6–induced Evans blue accumulation in the lung parenchyma. MTJ1 knockdown abolished protective effects of OxPAPC against vascular leak caused by IL-6 (Figure 7D). In an alternative model of ALI induced by HTV (Nonas *et al.*, 2008), control and si-MTJ-1–treated mice were exposed to HTV (30 ml/kg, 4 h) with or without OxPAPC administration. Measurements of BAL protein concentration and cell count in HTV-subjected animals showed no significant difference between nonspecific and si-MTJ-1–transfected groups (Figure 7E), whereas depletion of MTJ-1 abolished protective effects of OxPAPC against HTV-induced increases in BAL cell count and protein concentration as compared with controls transfected with nonspecific siRNA (Figure 7E).

DISCUSSION

A number of cell receptors interacting with oxidized phospholipids have been identified and shown to be involved in various cell responses, including proinflammatory and anti-inflammatory effects, immunity, angiogenesis, activation of gene expression, and lipid metabolism (Bluml *et al.*, 2005; Salomon, 2005; Bochkov *et al.*, 2010; Lee *et al.*, 2012). However, receptor(s) mediating barrier-protective effects of low OxPAPC doses remain elusive. Here we present the first report of a heat shock protein family member as a cell surface receptor mediating signaling by oxidized phospholipids.

Traditionally, GRP78 function as a molecular chaperone was associated with recognition of misfolded polypeptides, leading to stimulation of GRP78 activity as molecular chaperone and initiation of the unfolded protein response (Li and Lee, 2006; Dudek *et al.*, 2009). Alternative cell surface localization of ER-localized chaperone GRP78 was documented by immunofluorescence staining and cell surface biotinylation (Philippova *et al.*, 2008). However, GRP78 has never been considered as a mediator of phospholipid signaling.

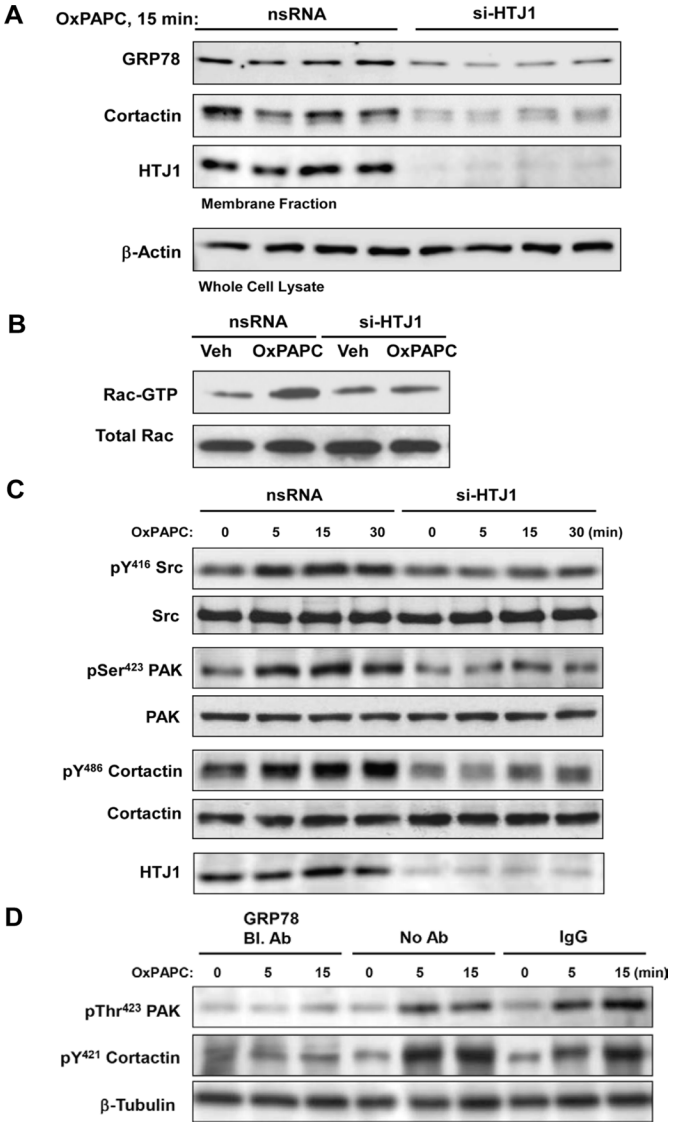

FIGURE 5: GRP78 and OxPAPC-induced activation of Rac signaling. HPAECs were treated with nonspecific or HTJ-11–specific siRNA before OxPAPC (10 μg/ml, 15 min) stimulation. (A) Effect of HTJ-1 knockdown on OxPAPC-induced membrane translocation of GRP78 and cortactin. HTJ-1 protein depletion was verified by Western blot. (B) Rac-GTP pull-down assay of control and HTJ-1–depleted HPAEC. (C) Effect of HTJ-1 knockdown on OxPAPC-induced site-specific phosphorylation of Src, PAK1, and cortactin. Autophosphorylation of Src at Tyr-416, indicating its activation, phosphorylation of Rac target PAK1 at Ser-423 and Ser-199, as well as cortactin phosphorylation at Tyr-421 and Tyr-486, reflecting activation of Rac signaling, were detected by immunoblotting. (D) Effect of HPAEC preincubation with GRP78-blocking antibody on OxPAPC-induced site-specific phosphorylation of PAK1 and cortactin. ECs were pretreated with GRP78-blocking antibody (50 μg/ml), vehicle, or control IgG before OxPAPC stimulation (10 μg/ml).

OxPAPC triggered HTJ-1–assisted accumulation of GRP78 at the cell membrane, which turned on GRP78/HTJ-1–mediated assembly of other components of the S1P-R1 signaling complex and their recruitment to the CEM, which provided full activation of S1P-R1 and downstream Rac pathway of EC barrier enhancement. OxPAPC binding to EC plasma membrane–resident GRP78 promoted recruitment of GRP78 to CEM. This induced cytosolic HTJ1/GRP78 complexes to be recruited to the plasma membrane and led to further recruitment of GRP78 to CEM, which potentiated transactivation of S1P-R1 and led to EC barrier enhancement. Although we have not elucidated the complete mechanism(s) of how plasma membrane–activated GRP78 recruits cytosolic GRP78 to the plasma membrane, our results demonstrate that HTJ1 is crucial for this process. Precise mechanisms of signal complex assembly in the CEM driven by OxPAPC-activated GRP78 require further investigation, but these data strongly suggest that in addition to acting as a molecular chaperone, GRP78 regulates OxPAPC cytoskeletal remodeling and EC barrier function by assembling the S1P-R1–Akt–mTOR–Tiam1/Vav-2–Rac1 signalosome.

Although we cannot exclude additional mechanisms of OxPLs barrier-protective effects—for example, disturbance of lipid bilayer structure or GRP78/HTJ-1 interactions with other receptors involved in EC barrier regulation—stable physical binding between GRP78 and OxPLs, which was demonstrated by different approaches (Figure 2), strongly supports the notion that GRP78 is a bona fide signaling receptor for OxPLs. We speculate that "hijacking" of the sphingosine-1-phosphate signaling mechanism by OxPAPC via prolonged transactivation of the S1P-R1 receptor defines the sustained endothelial barrier–enhancing response.

Potent anti-inflammatory effects of OxPAPC in models of acute inflammation have been associated with inhibition of inflammatory signaling induced by toll-like receptor 4 (TLR4) and TLR9. Administration of OxPAPC decreased inflammatory cell recruitment and even protected against endotoxin-induced lethal shock in animal models of acute inflammation (Bochkov *et al.*, 2002; Ma *et al.*, 2004; Nonas *et al.*, 2006; Erridge *et al.*, 2008; von Schlieffen *et al.*, 2009; Oskolkova *et al.*, 2010). This study is the first demonstration of the GRP78/HTJ-1–dependent mechanism of vascular barrier protection in two models of lung injury not directly associated with TLR receptor activation. Taken together, these findings expand our understanding of the role of OxPLs in innate immunity and control of tissue inflammation and show that OxPAPC activates at least two independent anti-inflammatory mechanisms— suppression of TLR-dependent inflammatory signaling (Bochkov *et al.*, 2002; Walton *et al.*, 2003) and GRP78–S1P-R1 mediated vascular barrier protection (present study).

In summary, we propose a mechanism of OxPAPC-induced EC barrier enhancement via GRP78/HTJ-1 acting as an OxPAPC/OxPAPS receptor (Figure 8). OxPAPC directly interacts with GRP78, which leads to membrane accumulation of the GRP78/HTJ-1 complex and its targeting to the CEM. Activated complex triggers Src/Fyn kinase activation, leading to assembly of Akt–PI3K–mTOR–S1P-R1 signalosome and transactivation of S1P-R1, which in turn activates the downstream Rac pathway, cortical actin cytoskeletal remodeling, and enhancement of the EC barrier. This study demonstrates a novel role of GRP78/HTJ-1 as a receptor mediating barrier-protective effects of oxidized phospholipids and engaged in assembly of CEM-associated signalosome, which is critical for maintenance of cell barrier homeostasis. These results provide a basis for further investigation into the roles of membrane-associated molecular chaperones in normal and pathological cell signaling.

MATERIALS AND METHODS

Reagents and cell culture

Unless specified, biochemical reagents were obtained from Sigma-Aldrich (St. Louis, MO). Antibodies to phosphocortactin and cortactin were from Millipore (Billerica, MA); GRP78, VE-cadherin, calnexin, calreticulin, and HTJ-1 were from Santa Cruz

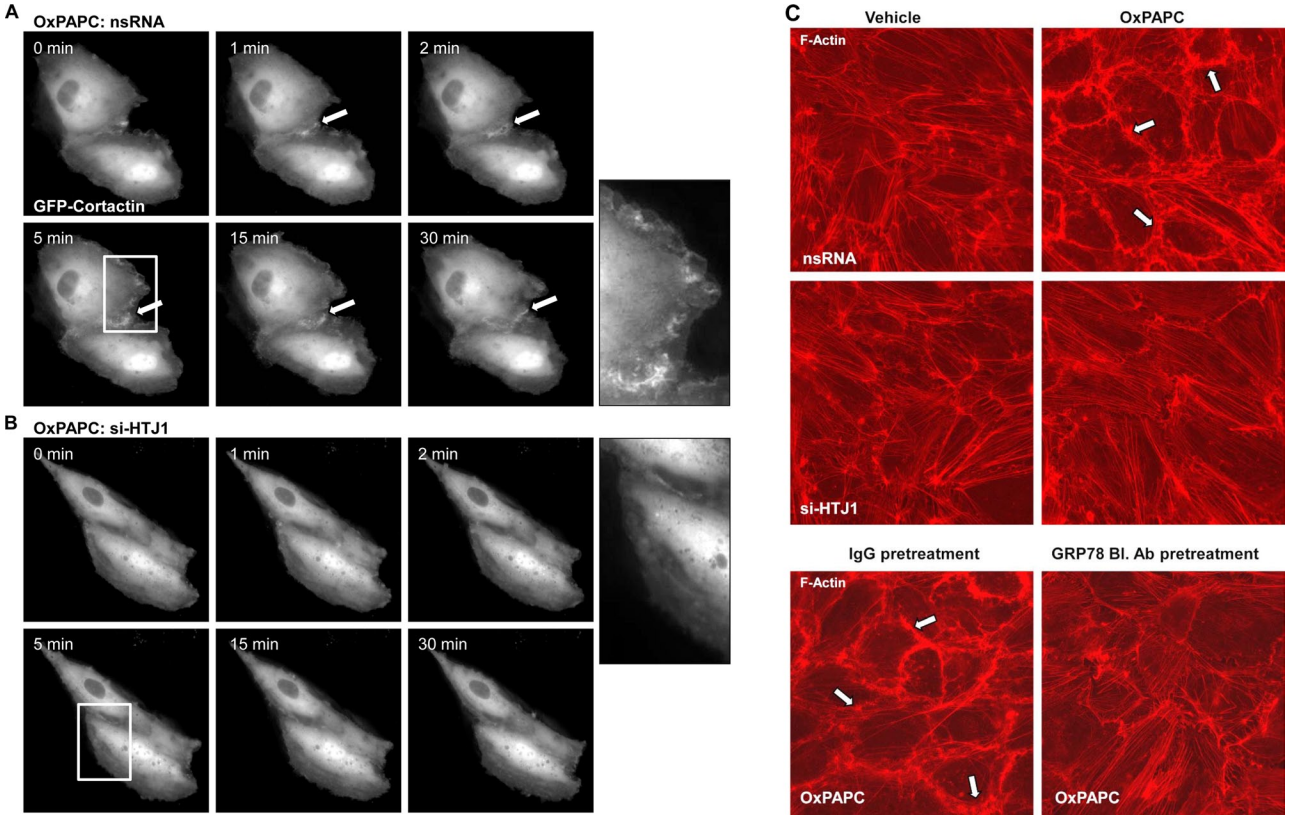

FIGURE 6: HTJ-1 knockdown blocks OxPAPC-induced activation of cortical actin dynamics and cortactin accumulation. (A) Live-cell imaging of HPAEC labeled with GFP-cortactin and stimulated with OxPAPC (10 μg/ml). Consecutive images were taken after 1, 2, 5, 15, and 30 min of OxPAPC stimulation. (B) OxPAPC-induced, time-dependent lamellipodia dynamics and peripheral cortactin accumulation were blocked by HTJ-1 knockdown. (C) HPAECs grown on glass coverslips were transfected with nonspecific or HTJ-1–specific siRNA (top) or incubated with control IgG or GRP78 blocking antibody (bottom), followed by OxPAPC stimulation (10 μg/ml, 30 min). Immunofluorescence staining with Texas red–phalloidin detects actin filaments. Arrows indicate peripheral F-actin enhancement caused by OxPAPC.

Biotechnology (Santa Cruz, CA); phospho-PAK1, phospho-Src, Src, Fyn, caveolin-1, and VEGFR2 antibodies were from Cell Signaling (Beverly, MA); GRP78 and Rac1 were from BD Transduction Laboratories (San Diego, CA), EO6 monoclonal antibody recognizing oxidized phosphatidyl choline epitope was from Avanti Polar Lipids (Alabaster, AL). Human pulmonary artery endothelial cells (HPAECs) and human lung microvascular endothelial cells were obtained from Lonza (Allendale, NJ).

Lipid oxidation and analysis

Nonoxidized PAPC was obtained from Avanti Polar Lipids. PAPC was oxidized by exposure to air for 36 h. The extent of oxidation was monitored by positive-ion electrospray mass spectrometry. Phospholipids were overlaid with argon and stored at –70°C.

siRNA and DNA transfections

Transfection of EC with siRNA was performed as previously described (Birukova *et al.*, 2010a). Predesigned HTJ-11– and MTJ-11–specific siRNAs of standard purity were purchased from Ambion (Austin, TX). After 72 h of transfection, cells were used for experiments. Transient transfection was performed using PolyJet reagent (SignaGen, Rockville, MD) according to the manufacturer's instructions. After 48 h of transfection, cells were treated with either vehicle or OxPAPC and used for live-imaging analysis. Plasmid encoding GFP-tagged cortactin was from Addgene (Cambridge, MA). For in vivo experiments, a predesigned MTJ-11–specific mouse siRNA set of standard purity was purchased from Ambion. Polymer-based administration of nonspecific or MTJ-11–specific siRNA conjugated with polycation polyethilenimine (PEI-22) was shown to promote lung-specific DNA and siRNA delivery (Thomas *et al.*, 2005a,b) and was used as described in our previous studies (Singleton *et al.*, 2009; Birukova *et al.*, 2010b). The optimal concentration of siRNA was determined in the following series of preliminary experiments. PEI-22-siRNA polyplexes were formed at a ratio of 1:10 (1 μg of siRNA/10 μg of PEI-22), and siPAK1 was tested in the 0.1- to 5.0-mg/kg dose range. SiRNA at 1–4 mg/kg showed the most significant inhibition of the target gene after 72 h of transfection, as determined by RT-PCR analysis of lung tissues or Western blot analysis (Figure 6A). Treated mice showed no signs of nonspecific siRNA-induced inflammation. Nonspecific, nontargeting siRNA (Dharmacon, Lafayette, CO) was used as a control treatment for both in vitro and in vivo experiments.

Transendothelial electrical resistance

TER across confluent human pulmonary artery endothelial monolayers was measured using an electrical cell-substrate impedance sensing system (Applied Biophysics, Troy, NY).

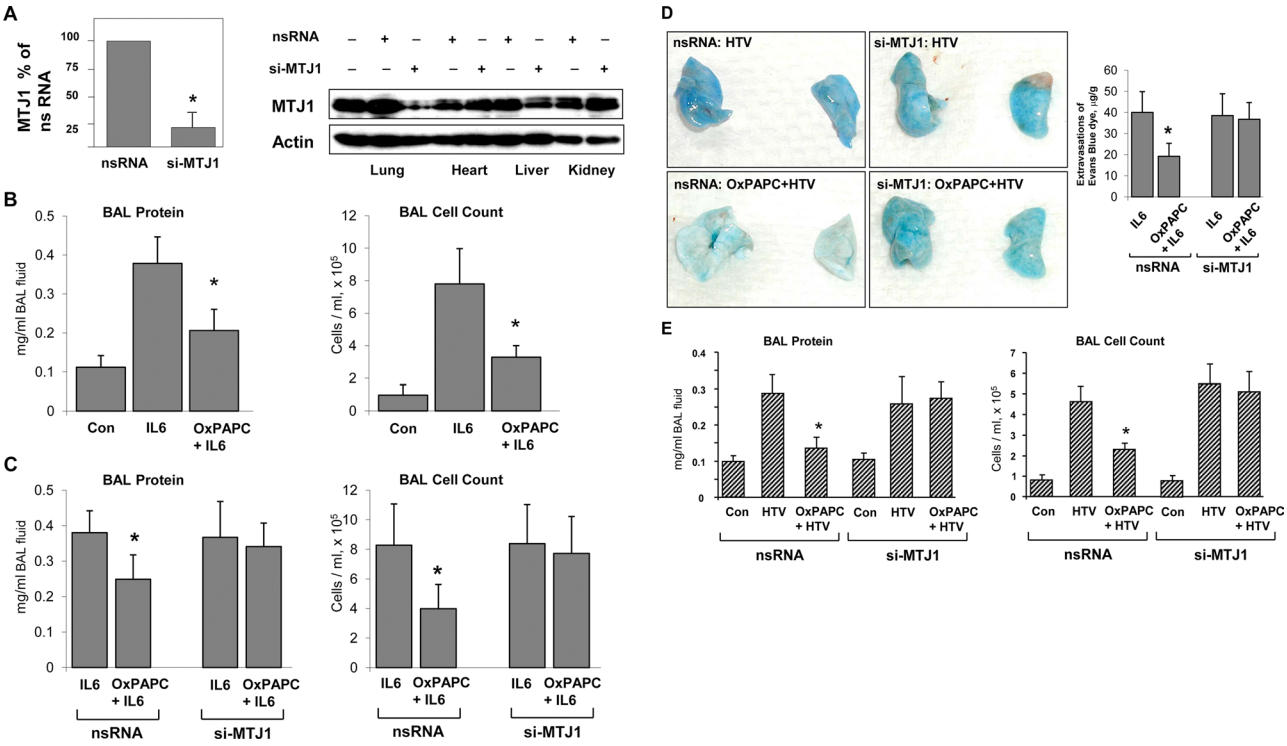

FIGURE 7: Knockdown of mouse homologue of HTJ-1 attenuates protective effects of OxPAPC in animal models of acute lung injury. Mice were transfected with nonspecific or MTJ-1–specific siRNA. (A) Tissue-specific MTJ-1 depletion was verified by RT-PCR analysis of lung samples and Western blot analysis of lung, heart, liver, and kidney extracts. (B) Protein concentration and cell count in BAL samples of control and IL-6–exposed mice (5 µg/kg, intrathecal) with or without OxPAPC treatment (1.5 mg/kg, intravenous; *$p < 0.05$ vs. IL-6; $n = 6$. (C, D) Mice were transfected with nonspecific or MTJ1-specific siRNA, followed by IL-6 administration with or without OxPAPC (1.5 mg/kg, intravenous). Protein concentration and cell count in BAL samples were analyzed. *$p < 0.05$ vs. IL-6; $n = 4$ (C). Vascular leak was assessed by measurements of Evans blue accumulation in the lung parenchyma. *$p < 0.05$ vs. nonspecific RNA; $n = 4$ (D). (E) Mice were transfected with nonspecific or MTJ1-specific siRNA, followed by HTV with or without OxPAPC intravenous injection (1.5 mg/kg). Protein concentration and cell count in BAL samples of control and HTV-exposed mice were analyzed. *$p < 0.05$ vs. HTV; $n = 6$.

GTPase activation, protein fractionation, immunoprecipitation, and immunoblotting

Activation of Rac GTPase in pulmonary endothelial cell culture was analyzed using a GTPase in vitro pull-down assay kit available from Millipore. Confluent HPAECs were stimulated with OxPAPC, and cytosolic and membrane fractions were separated using S-PEK kit (EMD Chemicals, Gibbstown, NJ). CEMs were isolated from human lung EC as previously described (Singleton *et al.*, 2009). Coimmunoprecipitation studies and Western blot analysis were performed using confluent HPAEC monolayers treated with vehicle or stimulated with OxPAPC. After stimulation, cells were lysed, and protein extracts were separated by SDS–PAGE, transferred to nitrocellulose membrane, and probed with specific antibodies.

Plasma membrane isolation protocol

Control and OxPAPC-treated endothelial cell lysates or CEM fractions were further purified to enrich plasma membrane–associated proteins by wheat germ agglutinin (WGA) affinity as previously described (Wang *et al.*, 2008; Singleton *et al.*, 2010). Briefly, cellular materials were solubilized in 50 mM 4-(2-hydroxyethyl)-1-piperazineethanesulfonic acid (pH 7.5), 150 mM NaCl, 20 mM $MgCl_2$, 1% Nonidet P-40 (NP-40), 0.4 mM Na_3VO_4, 40 mM NaF, 50 µM okadaic acid, 0.2 mM phenylmethylsulfonyl fluoride, and 1:250 dilution of Calbiochem protease inhibitor mixture 3 and added to WGA-conjugated agarose beads for 1 h at 10°C. The WGA beads were then centrifuged, the supernatant was removed, and precipitated proteins were eluted with 0.75 M *N*-acetylglucosamine containing 0.1% NP-40.

Surface protein biotinylation assay

Cells stimulated with OxPAPC were washed with phosphate-buffered saline (PBS; 37°C) and incubated with Sulfo-NHS-SS-Biotin (Pierce Biotechnology, Rockford, IL; 5 mM, 10 min, room temperature). Subsequently, cells were washed twice with 100 mM glycine/PBS, lysed in 1% Triton-100/PBS (30 min, on ice), and centrifuged (10,000 × g, 10 min, 4°C). Equal amounts of lysates were incubated with 60 µl of Streptavidin-agarose (Pierce Biotechnology, Rockford, IL; 1 h, 4°C). Beads were washed three times with ice-cold PBS and boiled in SDS sample buffer with 5% 2-mercaptoethanol. Samples were centrifuged for 1 min at 1000 × *g*, and supernatants were subjected to Western blotting with the antibody of interest.

Analysis of GRP78 interaction with OxPLs by gel electrophoresis

Sample preparation. Human recombinant GRP78 in PBS (30–100 ng) was mixed with OxPAPC, OxPAPS, DMPC, and DMPS (0.1–2 µg) in PBS/0.01% butylhydroxytoluene (total volume of 20 µl) overlaid with argon to prevent artificial oxidation. The mixture was incubated on a shaker for 90 min at 37°C.

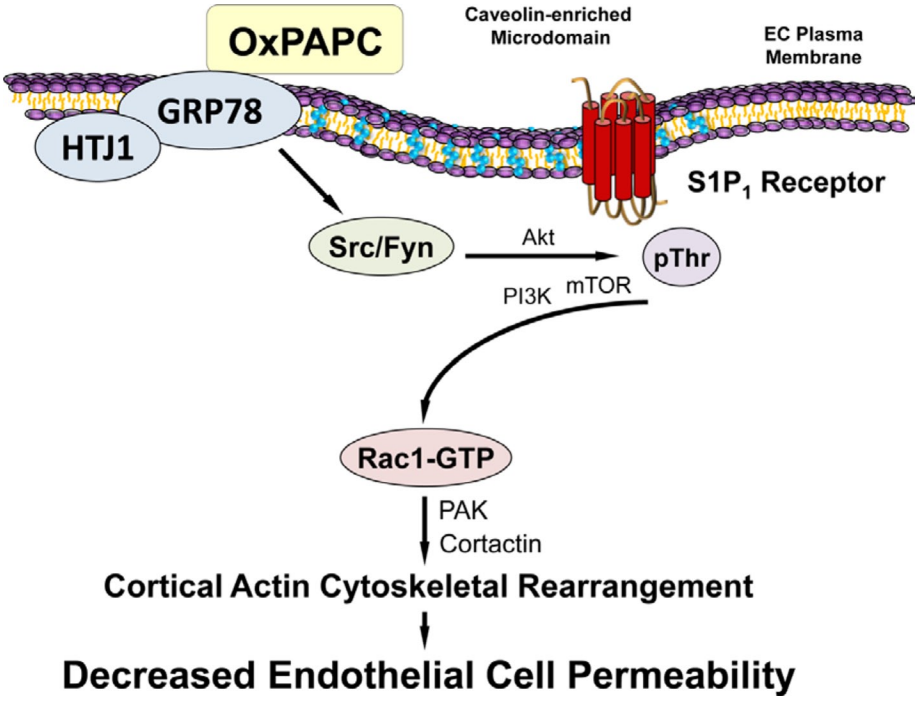

FIGURE 8: Proposed model of OxPAPC-induced human EC barrier enhancement. OxPAPC binds GRP78 and induces membrane localization of GRP78/HTJ-1 complex. OxPAPC-bound GRP78/HTJ-1 interacts with S1P-R1 and induces its activation via translocation to CEMs and consequent Src and Fyn tyrosine kinase–dependent phosphorylation of Akt, resulting in Akt-mediated S1P-R1 transactivation (threonine phosphorylation). Activated S1P-R1 receptor induces full activation of Akt via mTOR and PI3K-dependent serine and threonine phosphorylation required for Rac1 activation, cortical actin cytoskeletal rearrangement, and consequent OxPAPC-mediated EC barrier enhancement.

Band-shift assay. After addition of native PAGE sample buffer, samples were applied to a gradient 3–12% native PAGE gel (pH 7.5; Invitrogen) and run under nondenaturing conditions (50 mM Bis-Tris, 16 mM tricine, pH 7.3).

GRP78 ELISA

Microtiter 96-well plates (MaxiSorp; Nunc, Thermo Scientific, Rochester, NY) were coated with OxPAPS or DMPS (each 100 μg/ml in PBS containing 0.01% BHT) at 4°C overnight. Plates were washed with PBS and blocked with 3% bovine serum albumin (BSA) in PBS for 1 h at room temperature. Recombinant human GRP78 (Prospec-Tany Technogene, East Brunswick, NJ; 1 μg/ml in PBS/1% BSA) or HPAEC cell lysates in PBS/0.05% Tween-20 were applied for 1 h at room temperature. After washing with PBS and sequential addition of anti-GRP78 and anti-goat horseradish peroxidase (HRP) antibodies, one-step Ultra-TMB substrate (Thermo Scientific) was added. Absorption was measured using a 2030 Multilabel Reader Victor X5 (PerkinElmer, Waltham, MA).

Live-cell imaging and time-lapse tracking of cortactin dynamics

Cells were plated on MatTek dishes (MatTek, Ashland, MA) and transfected with GFP-cortactin. Images were acquired with a 100×/numerical aperture 1.45 oil objective in a 3I Marianas Yokogawa-type spinning disk confocal system equipped with a CO_2 chamber and a heated stage (Yokogawa, Tokyo, Japan). Time-lapse images were taken with 2-s intervals for 40-60 s.

Animal models and mechanical ventilation protocol

All experimental protocols involving the use of animals were approved by the University of Chicago Institutional Animal Care and Use Committee for the humane treatment of experimental animals. Ventilator-induced lung injury was performed as described previously (Birukova *et al.*, 2010a). In brief, C57BL/6J mice (8- to 10-wk-old males) with weight 20–25 g (Jackson Laboratories, Bar Harbor, ME) were anesthetized and subjected to mechanical ventilation (Harvard Apparatus, Boston, MA) at high tidal volume (30 ml/kg) for 4 h. In the other experimental group, C57BL/6J mice were randomized to concurrently receive sterile saline solution or IL-6 (5 μg/kg, intrathecal, 24 h) with or without subsequent exposure to mechanical ventilation.

Statistical analysis

Results are expressed as mean ± SD of four to six experiments. Experimental samples were compared with controls by unpaired Student's *t* test. For multiple-group comparisons, a one-way variance analysis and post hoc multiple comparisons tests were used. $p < 0.05$ was considered statistically significant.

ACKNOWLEDGMENTS

We thank Nicolene Sarich for excellent technical assistance with cell culture. This work was supported by grants from the National Institutes of Health (HL089257 and HL107920 to A.A.B.; HL076259 and HL087823 to K.G.B.) and the Fonds zur Förderung der Wissenschaftlicher Forschung (P22267-B11 to O.V.O. and P20801-B11 to V.N.B.).

REFERENCES

Birukova AA, Fu P, Chatchavalvanich S, Burdette D, Oskolkova O, Bochkov VN, Birukov KG (2007a). Polar head groups are important for barrier protective effects of oxidized phospholipids on pulmonary endothelium. Am J Physiol Lung Cell Mol Physiol 292, L924–L935.

Birukova AA, Fu P, Xing J, Yakubov B, Cokic I, Birukov KG (2010a). Mechanotransduction by GEF-H1 as a novel mechanism of ventilator-induced vascular endothelial permeability. Am J Physiol Lung Cell Mol Physiol 298, L837–L848.

Birukova AA, Malyukova I, Mikaelyan A, Fu P, Birukov KG (2007b). Tiam1 and betaPIX mediate Rac-dependent endothelial barrier protective response to oxidized phospholipids. J Cell Physiol 211, 608–617.

Birukova AA, Tian Y, Dubrovskyi O, Zebda N, Sarich N, Tian X, Wang Y, Birukov KG (2012a). VE-cadherin trans-interactions modulate Rac activation and enhancement of lung endothelial barrier by iloprost. J Cell Physiol 227, 3405–3416.

Birukova AA, Tian Y, Meliton AY, Leff AR, Wu T, Birukov KG (2012b). Stimulation of Rho signaling by pathologic mechanical stretch is a "second hit" to Rho-independent lung injury induced by IL-6. Am J Physiol Lung Cell Mol Physiol 302, L965–L975.

Birukova AA, Xing J, Fu P, Yakubov B, Dubrovskyi O, Fortune JA, Klibanov AM, Birukov KG (2010b). Atrial natriuretic peptide attenuates LPS-induced lung vascular leak: role of PAK1. Am J Physiol Lung Cell Mol Physiol 299, L652–L663.

Birukova AA, Zebda N, Cokic I, Fu P, Wu T, Dubrovskyi O, Birukov KG (2011). p190RhoGAP mediates protective effects of oxidized phospholipids in the models of ventilator-induced lung injury. Exp Cell Res 317, 859–872.

Bluml S *et al*. (2005). Oxidized phospholipids negatively regulate dendritic cell maturation induced by TLRs and CD40. J Immunol 175, 501–508.

Bochkov VN, Kadl A, Huber J, Gruber F, Binder BR, Leitinger N (2002). Protective role of phospholipid oxidation products in endotoxin-induced tissue damage. Nature 419, 77–81.

Bochkov VN, Oskolkova OV, Birukov KG, Levonen AL, Binder CJ, Stockl J (2010). Generation and biological activities of oxidized phospholipids. Antioxid Redox Signal 12, 1009–1059.

Bos CL, Richel DJ, Ritsema T, Peppelenbosch MP, Versteeg HH (2004). Prostanoids and prostanoid receptors in signal transduction. Int J Biochem Cell Biol 36, 1187–1205.

Chevalier M, Rhee H, Elguindi EC, Blond SY (2000). Interaction of murine BiP/GRP78 with the DnaJ homologue MTJ1. J Biol Chem 275, 19620–19627.

Dubrovskyi O, Birukova AA, Birukov KG (2013). Measurement of local permeability at subcellular level in cell models of agonist- and ventilator-induced lung injury. Lab Invest 93, 254–263.

Dudek J, Benedix J, Cappel S, Greiner M, Jalal C, Muller L, Zimmermann R (2009). Functions and pathologies of BiP and its interaction partners. Cell Mol Life Sci 66, 1556–1569.

Erridge C, Kennedy S, Spickett CM, Webb DJ (2008). Oxidized phospholipid inhibition of toll-like receptor (TLR) signaling is restricted to TLR2 and TLR4: roles for CD14, LPS-binding protein, and MD2 as targets for specificity of inhibition. J Biol Chem 283, 24748–24759.

Friedman P, Horkko S, Steinberg D, Witztum JL, Dennis EA (2002). Correlation of antiphospholipid antibody recognition with the structure of synthetic oxidized phospholipids. Importance of Schiff base formation and aldol concentration. J Biol Chem 277, 7010–7020.

Head JA, Jiang D, Li M, Zorn LJ, Schaefer EM, Parsons JT, Weed SA (2003). Cortactin tyrosine phosphorylation requires Rac1 activity and association with the cortical actin cytoskeleton. Mol Biol Cell 14, 3216–3229.

He F, Chen S, Wang H, Shao N, Tian X, Jiang H, Liu J, Zhu Z, Meng X, Zhang C (2011). Regulation of CD2-associated protein influences podocyte endoplasmic reticulum stress-mediated apoptosis induced by albumin overload. Gene 484, 18–25.

Horkko S *et al*. (1999). Monoclonal autoantibodies specific for oxidized phospholipids or oxidized phospholipid-protein adducts inhibit macrophage uptake of oxidized low-density lipoproteins. J Clin Invest 103, 117–128.

Imai Y *et al*. (2008). Identification of oxidative stress and Toll-like receptor 4 signaling as a key pathway of acute lung injury. Cell 133, 235–249.

Ishii H, Tezuka T, Ishikawa H, Takada K, Oida K, Horie S (2003). Oxidized phospholipids in oxidized low-density lipoprotein down-regulate thrombomodulin transcription in vascular endothelial cells through a decrease in the binding of RARbeta-RXRalpha heterodimers and Sp1 and Sp3 to their binding sequences in the TM promoter. Blood 101, 4765–4774.

Lee MJ *et al*. (2001). Akt-mediated phosphorylation of the G protein-coupled receptor EDG-1 is required for endothelial cell chemotaxis. Mol Cell 8, 693–704.

Lee S, Birukov KG, Romanoski CE, Springstead JR, Lusis AJ, Berliner JA (2012). Role of phospholipid oxidation products in atherosclerosis. Circ Res 111, 778–799.

Li J, Lee AS (2006). Stress induction of GRP78/BiP and its role in cancer. Curr Mol Med 6, 45–54.

Ma Z, Li J, Yang L, Mu Y, Xie W, Pitt B, Li S (2004). Inhibition of LPS- and CpG DNA-induced TNF-alpha response by oxidized phospholipids. Am J Physiol Lung Cell Mol Physiol 286, L808–L816.

Misra UK, Gonzalez-Gronow M, Gawdi G, Pizzo SV (2005). The role of MTJ-1 in cell surface translocation of GRP78, a receptor for alpha 2-macroglobulin-dependent signaling. J Immunol 174, 2092–2097.

Misra UK, Mowery Y, Kaczowka S, Pizzo SV (2009). Ligation of cancer cell surface GRP78 with antibodies directed against its COOH-terminal domain up-regulates p53 activity and promotes apoptosis. Mol Cancer Ther 8, 1350–1362.

Nakatsuka A *et al*. (2012). Vaspin is an adipokine ameliorating ER stress in obesity as a ligand for cell-surface GRP78/MTJ-1 complex. Diabetes 61, 2823–2832.

Nonas S, Birukova AA, Fu P, Xing J, Chatchavalvanich S, Bochkov VN, Leitinger N, Garcia JG, Birukov KG (2008). Oxidized phospholipids reduce ventilator-induced vascular leak and inflammation in vivo. Crit Care 12, R27.

Nonas SA, Miller I, Kawkitinarong K, Chatchavalvanich S, Gorshkova I, Bochkov VN, Leitinger N, Natarajan V, Garcia JG, Birukov KG (2006). Oxidized phospholipids reduce vascular leak and inflammation in rat model of acute lung injury. Am J Respir Crit Care Med 173, 1130–1138.

Oskolkova OV *et al*. (2010). Oxidized phospholipids are more potent antagonists of lipopolysaccharide than inducers of inflammation. J Immunol 185, 7706–7712.

Pfaffenbach KT, Lee AS (2011). The critical role of GRP78 in physiologic and pathologic stress. Curr Opin Cell Biol 23, 150–156.

Philippova M, Ivanov D, Joshi MB, Kyriakakis E, Rupp K, Afonyushkin T, Bochkov V, Erne P, Resink TJ (2008). Identification of proteins associating with glycosylphosphatidylinositol- anchored T-cadherin on the surface of vascular endothelial cells: role for Grp78/BiP in T-cadherin-dependent cell survival. Mol Cell Biol 28, 4004–4017.

Salomon RG (2005). Isolevuglandins, oxidatively truncated phospholipids, and atherosclerosis. Ann NY Acad Sci 1043, 327–342.

Shani G, Fischer WH, Justice NJ, Kelber JA, Vale W, Gray PC (2008). GRP78 and Cripto form a complex at the cell surface and collaborate to inhibit transforming growth factor beta signaling and enhance cell growth. Mol Cell Biol 28, 666–677.

Shi-Chen Ou D, Lee SB, Chu CS, Chang LH, Chung BC, Juan LJ (2011). Transcriptional activation of endoplasmic reticulum chaperone GRP78 by HCMV IE1-72 protein. Cell Res 21, 642–653.

Singleton PA, Chatchavalvanich S, Fu P, Xing J, Birukova AA, Fortune JA, Klibanov AM, Garcia JG, Birukov KG (2009). Akt-mediated transactivation of the S1P1 receptor in caveolin-enriched microdomains regulates endothelial barrier enhancement by oxidized phospholipids. Circ Res 104, 978–986.

Singleton PA, Mirzapoiazova T, Guo Y, Sammani S, Mambetsariev N, Lennon FE, Moreno-Vinasco L, Garcia JG (2010). High-molecular-weight hyaluronan is a novel inhibitor of pulmonary vascular leakiness. Am J Physiol Lung Cell Mol Physiol 299, L639–L651.

Soejima N *et al*. (2013). Intracellular accumulation of toxic turn amyloid-beta is associated with endoplasmic reticulum stress in Alzheimer's disease. Curr Alzheimer Res 10, 11–20.

Sokolowska I, Woods AG, Gawinowicz MA, Roy U, Darie CC (2012). Identification of potential tumor differentiation factor (TDF) receptor from steroid-responsive and steroid-resistant breast cancer cells. J Biol Chem 287, 1719–1733.

Thomas M, Ge Q, Lu JJ, Chen J, Klibanov AM (2005a). Cross-linked small polyethylenimines: while still nontoxic, deliver DNA efficiently to mammalian cells in vitro and in vivo. Pharm Res 22, 373–380.

Thomas M, Lu JJ, Ge Q, Zhang C, Chen J, Klibanov AM (2005b). Full deacylation of polyethylenimine dramatically boosts its gene delivery efficiency and specificity to mouse lung. Proc Natl Acad Sci USA 102, 5679–5684.

Thongtan T, Wikan N, Wintachai P, Rattanarungsan C, Srisomsap C, Cheepsunthorn P, Smith R (2012). Characterization of putative Japanese encephalitis virus receptor molecules on microglial cells. J Med Virol 84, 615–623.

von Schlieffen E *et al*. (2009). Multi-hit inhibition of circulating and cell-associated components of the toll-like receptor 4 pathway by oxidized phospholipids. Arterioscler Thromb Vasc Biol 29, 356–362.

Walton KA *et al*. (2003). Specific phospholipid oxidation products inhibit ligand activation of toll-like receptors 4 and 2. Arterioscler Thromb Vasc Biol 23, 1197–1203.

Wang Y, Ao X, Vuong H, Konanur M, Miller FR, Goodison S, Lubman DM (2008). Membrane glycoproteins associated with breast tumor cell progression identified by a lectin affinity approach. J Proteome Res 7, 4313–4325.

Weed SA, Parsons JT (2001). Cortactin: coupling membrane dynamics to cortical actin assembly. Oncogene 20, 6418–6434.

Wei PC *et al*. (2012). Loss of the oxidative stress sensor NPGPx compromises GRP78 chaperone activity and induces systemic disease. Mol Cell 48, 747–759.